The 12th IEEE International Workshop on Advanced Motion Control
March 25-27, 2012, Sarajevo, Bosnia and Herzegovina

Anti-sway Sliding-mode with Trolley Disturbance Observer for Overhead Crane system

Jadesada Maneeratanaporn
Department of System Design Engineering
Keio University
Yokohama 223-8522, Japan
Email: jadesada.m@gmail.com

Toshiyuki Murakami
Department of System Design Engineering
Keio University
Yokohama 223-8522, Japan
Email: mura@sd.keio.ac.jp

***Abstract*—Moving the suspended load along a predefined trajectory as fast as possible is not an easy controlling task due to the residual swing at the end of travelling. In this paper, the overhead crane is fully automated with the high speed trajectory. Robust scheme, namely anti-sway sliding-mode with trolley disturbance observer (DOB), are implemented with overhead crane systems. The anti-sway sliding-mode is specially designed for underactuated nonlinear systems which is derived from Lyapunov law. The asymptotic stability of switching function is proved theoretically. The controller can eliminate the error toward their sliding surfaces. Furthermore, trolley disturbance observer is also implemented to enhance the robustness.**

An obvious advantage of this kind of controller is based on simple control scheme however it can guarantee the robustness, speed convergence and swing suppression. In this paper, Experiment results are presented to show the superiority of the anti-sway sliding-mode with actuator's disturbance observer by comparing the effectiveness with PD controller assisting with Lyapunov based anti-sway controller and anti-sway sliding mode without disturbance observer. Not only that,but also the filtering technique is employed to eliminate chattering effect.

***Index Terms*—Overhead crane, Underactuated nonlinear systems, Anti-sway sliding-mode, Disturbance observer (DOB)**

I. Introduction and Motivations

Overhead crane are widely applied as a human-assist tools to deliver all kinds of bulky cargo in various locations such as industry, workshop and harbor . In the conventional crane operation, the crane's motion is mostly controlled by human. This manual operation depends on individual skill and experience, thus manufacturers are spending their effort to construct fully-automated drive systems which would achieve the optimum speed and successful task. This automatic systems will enhance the repeating task performance and yield higher production.

There are many favorable features for crane systems such as high payload ratio, high motion speed, safety, low economical cost and so on. However, the most crucial requirement is to optimum operation time, i.e. transporting the suspended payloads to the required position as fast and as precisely as possible without collision with other equipments. Thus, the payload swing angle at the end of motion should be minimized as possible [1]. Therefore, this control issue is very challenging and troublesome because the crane system is commonly effected by the effect of unmodeled system dynamics and environmental disturbance like wind. Therefore, the idea of anti-sway controller has been developed by many researchers.

Since late of twentieth century, there are many approaches to deal with the crane systems. They firstly used the time optimal control but with no considering about hoisting motion [2]. A bang bang control, with the fixed rope length, was also conducted by [3]. Mita [4] derived the crane in five different sections and derive the optimal speed reference trajectory which maximizes a quadratic cost function. But in their works focused on the the swing of load rather than traveling time, thus it takes longer time than other optimizaion methods. The time optimal control for diagonal trajectory, while using linearized model, was investigated in [5]. Then, Yamamoto[6] investigated a maximum velocity profile with hoisting system.

Besides optimal control, the other approaches generally based on matched system model and linearization. [7] adopted input shaping control method which is strongly based on system model. These approaches lacked robustness to external disturbances and could not damp residual swing well. Moreover, zero initial condition is required. [8] offered observer/controller design based on Lyapunov equivalence while requiring precise system model and complex matrix computation .

Likewise, the mentioned controller emphasized on anti-sway at the end of motion which might lead to lack of safety along the load transmission. Also the effect of external disturbance such as wind and parameter uncertainty in unmodeled system. As the consequence, these issues triggered the robust control approach.

Specifically, SMC is commonly used in various nonlinear systems. However, the traditional SMC cannot be implemented directly to crane system. Since the system has two degree of freedoms (horizontal movement and sway angle) but has only one control inputs (trolley force). There are previous researches, focused on SMC with underactuated systems. A hierarchical sliding-mode control [9] proves the switching function of the whole system and each subsystem are asymptotically stable, but it does not guarantee the convergence speed of the switching function of each subsystem. Lee [10] presented an anti-swing control by employing a switching function that couples load-dynamics with trolley motion for

978-1-4577-1073-5/12/$26.00 ©2012 IEEE

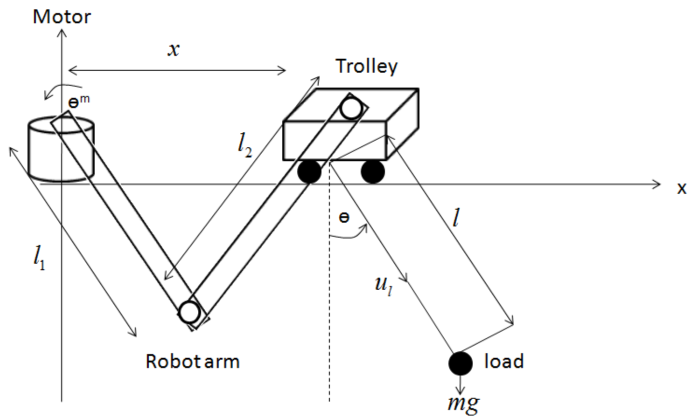

Fig. 1. Model of an overhead crane

stability of load-swing dynamics. The most appealing for his research is model-following trajectory which claimed to reduce the swing angle compare with any trajectories. His result was verified by experiment.

In this paper, the new switching function is designed, for instance, Lee's controller is slightly modified to increase the convergence speed . Moreover, trolley DOB are also applied to extend the SMC performance. Some sliding mode robustness issues are during the transient period the controlled system may be sensitive to parameter variations and disturbances because the sliding mode is not realized and the another issue is in the case of the model uncertainties are higher than switching gain of SMC, the system state will not converge to surface. Thus, DOB helps sliding mode more easier to implement in practical usage [11],[12]. Moreover, the filtering technique [13],using lowpass filter with variable bandwidth, is also employed to reduce chattering effect. The structure of this paper is arranged as follow. Section II contains System Description preliminaries necessary for analyzing and designing an appropriate controller. The control algorithms are illustrated in Section III, i.e. sliding mode with anti-sway, disturbance observer and filtering technique. A comparison of these control methods are presented in Section IV through experimental results. Finally, in the last Section V, some conclusions are briefly drawn and also the future works are illustrated.

II. System Description

A. Crane dynamics

According to the crane model in Fig. 1, shows the model of an overhead crane and its suspended load. The system is classified as the underactuated systems, i.e. the number of outputs is larger than the number of inputs.

In addition, the system has two degrees of freedom which are displacement of trolley in x-direction (x, m), suspended load's swing angle (θ, radian). On the other hand, for the input, the trolley is driven by a x-direction force (u_x, N). Thus, using the Lagrange mechanics, the equations of motion was derived by Lee [14] are obtained as

$$(m_x+m)\ddot{x}+ml\cos\theta\ddot{\theta}+d_{vx}\dot{x}-ml\sin\theta\dot{\theta}^2=u_x \tag{1}$$

$$l\ddot{\theta}+\cos\theta\ddot{x}+g\sin\theta=0 \tag{2}$$

where m is the load mass, m_x is the equivalent masses of the rotating parts such as motors and their drive trains; d_{vx}represents the viscous damping coefficients associated with the x ; g represents the gravitional acceleration.

To design the sliding mode in the control section III, we have to rearrange dynamics equation to this following form and also concern the disturbance[15];

$$\ddot{x} = f_x(q,\dot{q})+b_x(q,\dot{q})u_x+D_x \tag{3}$$

where

$$\begin{aligned} f_x(q,\dot{q}) &= \frac{-ml\cos\theta\ddot{\theta}-d_{vx}\dot{x}+ml\sin\theta\dot{\theta}^2}{m_x+m} \\ b_x(q,\dot{q}) &= \frac{1}{m_x+m} \end{aligned} \tag{4}$$

where D_x is the disturbance acting on sway motion and horizontal direction, Note that to obtain (3), we rearrange the $\ddot{x}$ to one side of the equation.

In practical, mismatch parameter should be considered, thus rewritten in the form of nominal parameter and uncertainties as follows;

$$\begin{aligned} \ddot{x} &= \tilde{f}_x(q,\dot{q})+\Delta f_x(q,\dot{q})+\tilde{b}_x(q,\dot{q})u_x+\Delta b_x(q,\dot{q})u_x+D_x \\ &= \tilde{b}_x(q,\dot{q})u_x+{D^*}_x \end{aligned} \tag{5}$$

where ${D_x}^* = \tilde{f}_x(q,\dot{q})+\Delta f_x(q,\dot{q})+\Delta b_x(q,\dot{q})u_x+D_x$, $\tilde{\bigcirc}$ indicates nominal term and Δ indicates uncertainty term.

B. Actuator dynamics

Practically, crane system (II-A) is drived by the electromechanical actuator. Actuator dynamics are described as follows;

$$J_m\ddot{\theta}_a = T_m-D\dot{\theta}_a-T_{dis} \tag{6}$$

$$T_m = K_tI_a \tag{7}$$

$$\theta_a = G_r\theta^m \tag{8}$$

$$T = G_rT_m \tag{9}$$

where θ_a is motor rotation angle $[rad]$, J_m is motor axis inertia $[kgm^2]$, D is friction coefficient $[Nmrad/s]$, T_m is motor torque $[Nm]$, K_t is torque constant $[Nm/A]$, I_a is electricity current $[A]$, T_{dis} is disturbance torque, θ^m is motor output angle $[rad]$ and G_r is gear ratio. Then rearrange (6) by substituting (8) and (9), thus (6) becomes (10) and also substitute (7) into (9), it results in (11);

$$G_rJ_m\ddot{\theta}^mG_r+G_rD\dot{\theta}^mG_r+G_rT_{dis}=T \tag{10}$$

$$T=G_rK_tI_a \tag{11}$$

C. Coordinate Transfomation And Control Input Transformation

In this section, forward kinematic and Jacobian are introduced. Forward kinematic is used for transforming angular coordinate to planar coordinate as shown in (12). Jacobian is used for converting angular velocity to planar velocity as shown in (13). In addition, angular coordinate in this experiment is considered as motor angle. On the other hand, planar coordinate is considered as trolley position as shown in Fig. 1, forward kinematic can be calculated as follows.

$$fw(\theta^m)=\sqrt{{l_2}^2-{l_1}^2\cos^2(\theta^m)}+l_1\sin(\theta^m) \tag{12}$$

Taking derivative both sides of (12);

$$Jaco(\theta^m) = \frac{l_1\cos(\theta^m) + {l_1}^2\cos(\theta^m)\sin(\theta^m)}{\sqrt{{l_2}^2 - {l_1}^2\cos^2(\theta^m)}} \quad (13)$$

To sum up the relationships between planar coordinate and angular coordinate is illustrated as follows;

$$\begin{aligned} x &= fw(\theta^m) && (14)\\ \dot{x} &= Jaco(\theta^m)\dot{\theta}^m && (15)\\ \ddot{x} &= Jaco(\theta^m)\ddot{\theta}^m + \dot{J}aco(\theta^m)\dot{\theta}^m \\ &\approx Jaco(\theta^m)\ddot{\theta}^m && (16)\end{aligned}$$

In practical, force u_x must be converted to motor angular reference $\ddot{\theta}^m_{ref}$ by following procedure, Recall (5) and define acceleration refence as $\ddot{x}_{ref}$;

$$\ddot{x}_{ref} = \tilde{b}_x(q,\dot{q})u_x + D^*{}_x \quad (17)$$

Dividing $Jaco(\theta^m)$ both sides of equation;

$$Jaco^{-1}(\theta^m)\ddot{x}_{ref} = Jaco^{-1}(\theta^m)\tilde{b}_x(q,\dot{q})u_x + D^*{}_x \quad (18)$$

Now (18) can be rewritten as;

$$\ddot{\theta}_{ref} = \tilde{b}_x T + D^*{}_x \quad (19)$$

$$\tilde{b}_x^{-1}\ddot{\theta}_{ref} - \tilde{b}_x^{-1}D^*{}_x = T \quad (20)$$

Combine crane dynamics (20) with actuator dynamics (10), yield to (21);

$$\begin{aligned}&(G_rJ_mG_r + \tilde{b}_x^{-1})\ddot{\theta}_{ref} + G_rD\dot{\theta}^mG_r && (21)\\ &\quad + G_rT_{dis} - \tilde{b}_x^{-1}D^*{}_x = T\end{aligned}$$

Define nominal Total inertia as $\tilde{M}$ and total actuator disturbance as $T^*{}_{dis}$ whose value is $G_rD\dot{\theta}^mG_r + G_rT_{dis} - \tilde{b}_x^{-1}D^*{}_x$ Thus the final equation will be;

$$(\tilde{M})\ddot{\theta}_{ref} + T^*{}_{dis} = G_r\tilde{K}_tI_a \quad (22)$$

This equation will be used for driving crane system and also for designing actuator disturbance observer in section III-B.

III. Control Algorithms

A. Sliding Mode Control with Anti-sway

A sliding mode control is classified as variable control structure control (VSC) whose structure between the switching surfaces is adapted to obtain the system's robustness. Thanks to this switching control, sliding-mode control can resist the internal parametric uncertainty and external disturbance. Simply speaking, the system dynamics is changed along particular surface in state space, thus the states of system can properly converge to the surface. During the sliding behavior, the system remains insensitive to parameter variations and external disturbances. As mentioned, overhead crane system is categorized as nonlinear coupled underactuated systems, which has single-input and two outputs. To construct suitable switching function for this underactuated system. The swing-dependent term is added, the proof of sway angle is refered to Appendix [17] and also add integral term for compensating steady state error and term k_xs_x to improve the convergence speed;

$$s_x = c_xe_x + \dot{e}_x + k_i\int e_x dt - c_\theta e_\theta \quad (23)$$

After injecting damping sway term in the switching function and integral term, the stability prove is similar to traditional sliding mode

$$V(t) = \frac{1}{2}{s_x}^2 \quad (24)$$

Differrentiate by time both sides of the equation;

$$\begin{aligned}\dot{V}(t) &= s_x\dot{s}_x\\ &= s_x(k_ie_x + c_x\dot{e}_x - c_\theta\dot{e}_\theta + \ddot{e}_x)\\ &= s_x(k_ie_x + c_x\dot{e}_x - c_\theta\dot{e}_\theta + \ddot{x} - \ddot{x}_{cmd})\\ &= s_x(k_ie_x + c_x\dot{e}_x - c_\theta\dot{e}_\theta + \tilde{b}_x(q,\dot{q})u_x\\ &\quad + {D_x}^* - \ddot{x}_{cmd}) && (25)\end{aligned}$$

Let $D_{sx} = k_ie_x + c_x\dot{e}_x - c_\theta\dot{e}_\theta + {D_x}^*$; Substitute D_{sx} in (25), leads to (26);

$$\dot{V}(t) = s_x(\tilde{b}_x(q,\dot{q})u_x + D_{sx} - \ddot{x}_{cmd}) \quad (26)$$

Set the term $\tilde{b}_x(q,\dot{q})u_x = \ddot{x}_{cmd} - \eta_x\mathrm{sgn}(s_x) - k_xs_x$,while $\eta_x$and k_x are positive constants, so the u_x is ultimately obtained as;

$$u_x = \frac{\ddot{x}_{cmd} - \eta_x\mathrm{sgn}(s_x) - k_xs_x}{\tilde{b}_x(q,\dot{q})} \quad (27)$$

Practically, if the controller used the discontinuous high frequency as traditional $sgn(s_x)$, the actuator becomes risky to turn down, namely chattering effect. Consequencely, this smoother function is implemented. so that $sgn(s_x)$ is defined as following function;

$$\mathrm{sgn}(s_x) = \frac{s_x}{|s_x| + \delta} \quad (28)$$

where δ has positive value whose value is set as 0.0004 in this research.

Then,(27) is substituted back into (26), yields (29);

$$\begin{aligned}\dot{V} &= -\eta_x|s_x| - k_x{s_x}^2 + s_xD_{sx}\\ \dot{V} &\le -\eta_x|s_x| - k_x{s_x}^2 + |s_x||D_{sx}| && (29)\end{aligned}$$

Let $D_{xm} = \sup_{t\ge0}|D_{sx}|$ while $\eta_x > D_{xm}$, then (29) becomes;

$$\begin{aligned}\dot{V} &\le -k_x{s_x}^2 - |s_x|(\eta_x - |D_{sx}|)\\ \dot{V} &\le -k_x{s_x}^2 - |s_x|(\eta_x - D_{xm}) \le 0 && (30)\end{aligned}$$

As (30), the switching function is stable. Furthermore, $\dot{V}(t) \equiv 0$ is sastisfied when only null solution can be solved. Thus, switching function is asymptotically stable as referred from LaSalle's Theorem [16].

B. Trolley Disturbance Observer

To enhance the robustness of the systems, Disturbance observer is implemented in motor control current. Although switching control in sliding mode can handle with external disturbance and parameter uncertainties, but in practical the disturbance in actuator dynamics should be compensated for higher robustness.

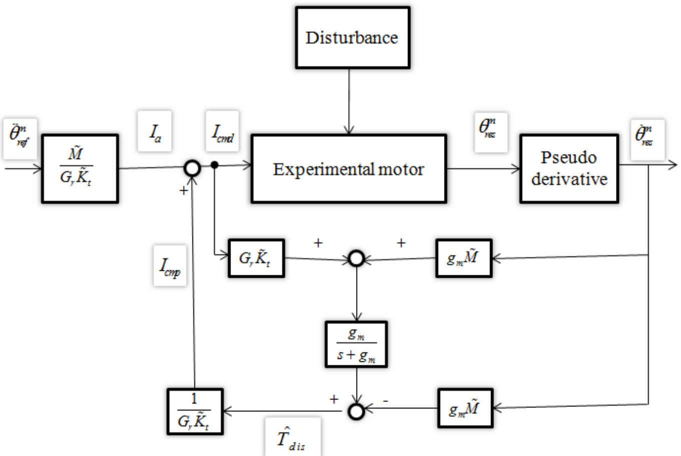

Fig. 2. Block diagram of Actuator's disturbance observer

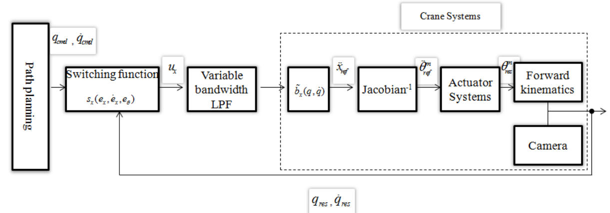

Fig. 3. Block diagram (simplified).

TABLE I
EXPERIMENTAL PARAMETERS

$\tilde{m}_x$	Travelling components' mass[kg]	3.0
$\tilde{m}$	Load mass [kg]	1
g	Acceleration of gravity[m/s^2]	9.807
l	Constant rope length[m]	0.64
$\tilde{d}v_x$	Damping coefficient with trolley motion [kg/s]	2.5
$\tilde{M}$	Total inertia of the systems [kgm/s^2]	0.5
l_1	Length of robot arm link1 [m]	0.77
l_2	Length of robot arm link2 [m]	0.8
t_{tra}	Traveling phase period[sec]	5.4
t_{arr}	Arrival phase period[sec]	9.6
t_0	Initial time[sec]	1.0
t_1	Ramp up duration[sec]	1.7
t_2	Traversing time[sec]	1.0
t_3	Ramp down duration[sec]	1.7
$\dot{x}^{\max}_{cmd}$	Maximum trolley velocity [m/s]	0.4
$\ddot{x}^{\max}_{cmd}, \ddot{x}^{\min}_{cmd}$	Maximum/minimum trolley acceleration [m/s^2]	0.23,-0.23
g_m	Cut-off frequency of $\hat{T}_{dis}$	5.0
k_f	gain of bandwidth for LPF	1500
k_x	Sliding mode gain for trolley systems	5.45
k_i	Integral gain	0.05
η_x	Switching gain for trolley systems	5.45
c_θ	Swing angle feedback gain	3.54
c_x	Trolley feedback gain	3.0
K_t	Torque constant [Nm/A]	10.3
G_r	Gear ratio	1/50

Explicitly, actuator disturbance observer ($\hat{T}_{dis}$) can be computed as follows; Recall the total dynamics from (22) section III-A and rewritten the equation as follows;

$$T^*{}_{dis} = G_r \tilde{K}_t I_a - (\tilde{M})\ddot{\theta}_{res} \tag{31}$$

$T^*{}_{dis}$ can be approximated by $\hat{T}_{dis}$, $\hat{T}_{dis}$can be obtained in the form of first order low pass filter as shown below;

$$\begin{aligned} \hat{T}_{dis} &= \frac{g_m}{s+g_m}(G_r \tilde{K}_t I_a - (\tilde{M})\ddot{\theta}_{res}) \\ &= \frac{g_m}{s+g_m}(G_r \tilde{K}_t I_a + g_m(\tilde{M})\dot{\theta}_{res}) - g_m(\tilde{M})\dot{\theta}_{res} \end{aligned} \tag{32}$$

where g_m is cut off frequency of low pass filter for $\hat{T}_{dis}$ To sum up, the block diagram of this observer is illustrated in Fig.(2).

C. Filtering Technique

One of the major problem of sliding mode control is chattering effect. In addition chattering effect can cause torque pulsation, current harmonics and acoustic noise. To compensate this drawback while the overall performance is maintained as great as non-compensated controller, the lowpass filter with variable-bandwith is employed. The structure of this filter is written as follows [13];

$$\frac{output}{input} = \frac{g_f}{s+g_f} \tag{33}$$

where $g_f = k_f\,|s_x|$, g_f is the cutoff frequency which varies to the magnitude of switching function. $input$ is set as unfiltered controller from III-A and $output$ is filtered controller.

IV. Experimental Results

To approve those theories as mentioned, the practical experiment has been carried out. It was designed by C language and RTLinux which is operated on personal computer, using Intel Pentium4 2.0 GHz. And the sway angle is captured by PSD camera. For the ease of comprehension, the overall system is simply shown in block diagram as shown in Fig.(3). Note that the controlling and system description are discussed in previous section. For the trolley trajectory, the trajectory is divided into two phase; 1.) traveling phase: Linear segments with parabolic blends (LSPB), whose has trapezoidal velocity profile was applied, this profile is appropriate when a constant velocity is desired along portion of the path [18]. The traveling phase is also consisted of three parts; ramp up, constant velocity and ramp down. 2.) The arrival phase: when the trolley reach the final position, the position is held as final value, velocity and acceleration are set to be zero. This phase is applied for stabilzing the sway angle. The trajectory, velocity and acceleration profile for this experiment are illustrated in Fig. 4- 6. Moreover, the sway angle command was set according to crane dynamics (2) as Lee proposed in [10]. The sway angle trajectory is illustrated in Fig. 7.

Furthermore, the experiment was categorized by control cases;
Case 1 Sliding mode
Case 2 Sliding mode with high gain (switching gain is set two time higher than case 1)
Case 3 PD controller with Lyapunov based antisway controller and flatness
Case 4 Sliding mode with $\hat{T}_{dis}$
Case 5 Flitered Sliding mode with $\hat{T}_{dis}$

Note that, for all cases, the rope length is set as constant as the limitation of hardware. Case 3 is the approach referred to Ishino [19](this approach is used for comparison only and not be discussed in this paper).

The goal of this research is to reach the final position with the most minimized time along with unnoticeable sway angle.

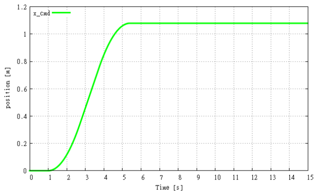

Fig. 4. Position profile

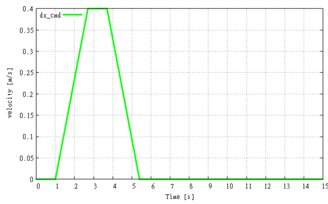

Fig. 5. Velocity profile

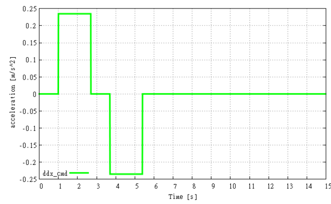

Fig. 6. Acceleration profile

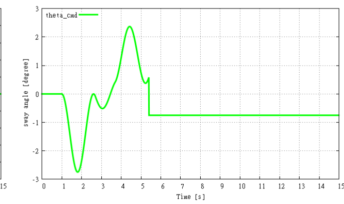

Fig. 7. Sway angle profile

Thus, the high speed trajectory is implemented in all cases. All the experimental parameters are illustrated in Table I.

According to Fig. 8- 12,the graphical results illustrate how well the trolley systems and track the designed trajectory path. Moreover, for the ease of analysis, the position errors and sway angle response from each controller are compared in Fig. 14 and Fig. 15. For Fig. 14, the graphical results indicate the difference between command trajectory and actual trajectory. For Fig. 15, all angle responses of this experiment are plotted. Not only the error response is considered, the chattering effect is also investigated as shown in Fig. 16. Because the graphical responses are insufficient to compare and analyze. The maximum overshoot, steady state error and magnitude of swing angle are analyzed. In addition, maximum overshoot is the peak of error response during traveling phase. The steady state error is observed when error become constant in arrival phase. And magnitude of swing angle is noted as the peak to peak of angle during the arrival phase [10-15 sec]. This additional error comparison for all cases is illustrated in Table II. The discussion was described by following categories;

1. Overall motion

Case 2- Case 5 can track command trajectory with small sway angle at the end of motion. However, case 1. can be obviously observed the huge error at the end of motion. Because the nonlinear switching gain of controller is not high enough to compensate the external disturbance. So case 1 will be considered as unsuccessful controller and will be neglected for further analysis.

Note that because of this result, switching gain (η_x) of case 2 is set to be twice as case 1 to observe the high gain's response. By the way, the other cases η_x is maintained to be the same as case 1.

2. Swing angle (Travelling phase and Arrival phase)

- Traveling phase: Case 3 has the least magnitude. Case 2 has the highest oscillation. Case 4 and case 5 has the same result
- Arrival phase: This phase can be infered as steady state. The angle from Case 3 has the highest oscillation at this phase. Case 2 has oscillation but the oscillation becomes unnoticable at the end of motion. Case 4 and case 5 has the same result and has the fastest convergence since the sway angle becomes unnoticable since tenth second.

3. Position error (Travelling phase and Arrival phase)

- Traveling phase: Case 2 has the highest maximum overshoot. Case 3,4 and 5 have slightly the same maximum overshoot.
- Arrival phase: The steady state error from case 3 has the highest value, about 2 times higher than case 2. And case 2 has steady state error about 5 times higher than case 4 and case 5. Explicitly, the steady state error is reduced because of integral term in sliding mode controller (case 2,4 and 5). Furthermore, the stability of whole system can be observed via sliding function as shown in Fig. 13, the results correspond to the position error and swing angle.

TABLE II
ERROR RESULTS

Control approach	Maximum Overshoot [m]	Steady state error [m]	Swing angle (peak to peak) [degree]
Case 1	0.7	0.2	1.7
Case 2	-0.376	-0.005	0.65
Case 3	-0.022	-0.01	0.5
Case 4	-0.019	-0.001	0.001
Case 5	-0.02	0.001	0.002

4. Motor current input

Three cases of sliding mode control are compared. Case 2 has the highest chattering due to high switching gain. Case 4 has less magnitude but chattering still occured. Case 5 has no chattering as the current input becomes continuous. This result can be inferred that low pass filter with variable bandwidth can reduce the chattering while preserves the robustness.

V. Conclusions and Future Works

This paper implements anti-sway sliding-mode with disturbance observer algorithm for controlling the motion of the nonlinear underactuated overhead crane system. The trapezoidal velocity is used as trajectory paths for the trolley. This experiment focuses on the safety and fast operation. Thus, the arrival phase is majorly focused, i.e as soon as load stops swinging and reaches the final position precisely, crane is able to continue to the next task. Correspond to the experimental results with the robustness investigation, The proposed method, Flitered Sliding mode with $\hat{T}_{dis}$, has the greatest performance in the term of position error reduction, sway angle reduction and also chattering free. From this research, some problems are found out and listed in future work as follows ;

- Maintenancing the actuator of hoisting system, thus systems becomes flexible rope length.
- Reducing chattering effects when the sliding mode encounter with strong disturbances or huge uncertainties by using high order sliding mode.
- Applying adaptive DOB to enchance the tracking error performance.

References

[1] Diantong Liu a, Jianqiang Yi, Dongbin Zhao, Wei Wang "Adaptive sliding mode fuzzy control for a two-dimensional overhead crane", *IEEE international Conference on Robotics and Automation*, 2547-2552, 2001

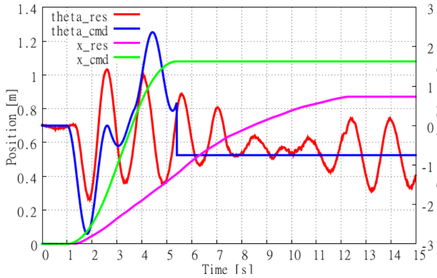

Fig. 8. Case 1: Using Sliding mode

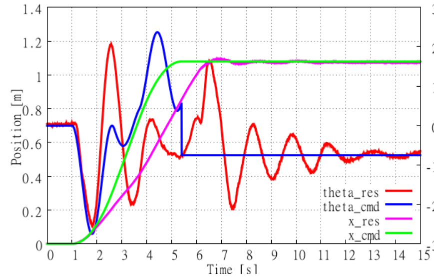

Fig. 9. Case 2: Using High gain with out DOB

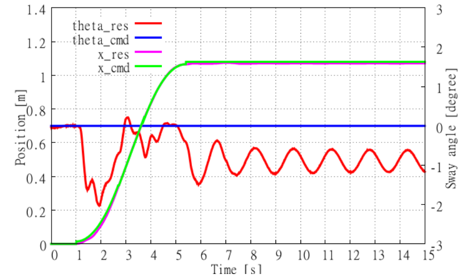

Fig. 10. Case 3: PD controller with Lyapunov based antisway controller and flatness

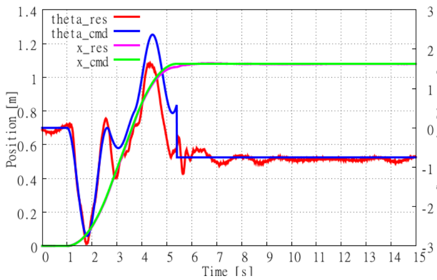

Fig. 11. Case 4: Sliding mode with $\hat{T}_{dis}$

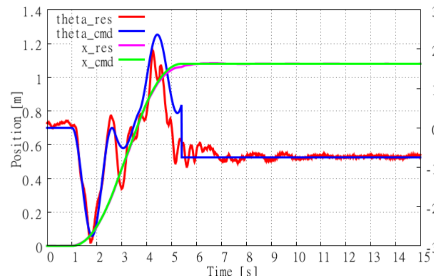

Fig. 12. Case 5: Filtered Sliding mode with $\hat{T}_{dis}$

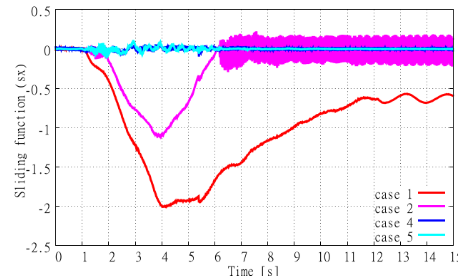

Fig. 13. Sliding function comparison

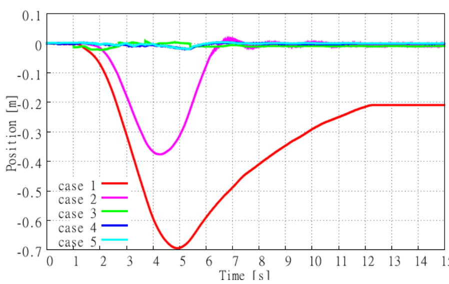

Fig. 14. Position error comparison

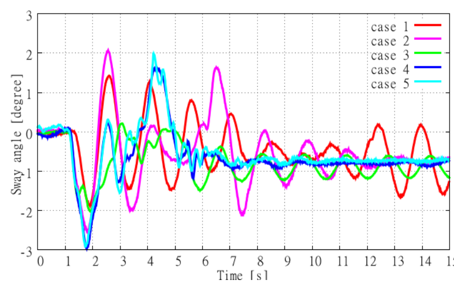

Fig. 15. Sway angle comparison

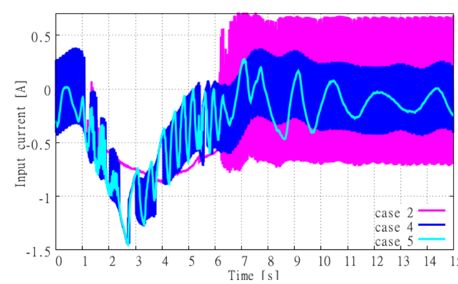

Fig. 16. Current input comparison

[2] Manson, G.A. "Time Optimal Control Methods Arising from the Study of Overhead Cranes", *Ph.D. Thesis, Univ. of Strathclyde*, 1977

[3] Mita, T. and Kanai "Optimal Control of the Crane System Using the Maximum Speed of the Trolley", *Trans. Soc. Instrum. Control Engr.*, Vol.15, No.6 (1979), p.833-838

[4] Sakawa, Y. and Shindo, Y. "Optimal Control of Container Cranes", *Automatica*, Vol.18, No.3 (1982), p.257-266

[5] Auernig, J.W. and Troger, H. "Time Optimal Control of Overhead Cranes with hoisting of the load", *Automatica*, Vol.23, No.4 (1987), p.693-707

[6] Yamamoto, T. and Momose, N. "A Swing Pendulum Control of the Trolley Crane with Variable Rope Length", *Trans Jpn. Soc. Mech Eng*, Vol.65, No.633 C (1999), p.1787-1793

[7] Singhose W, Porter L, Kenison M, Kriikku E. " Effects of hoisting on the input shaping control of gantry cranes.", *Control Eng Practice*, 2000, 8(10), p.1159-1165

[8] Giua A, Seatzu C, Usai G. "Observer-controller design for cranes via Lyapunov equivalence", *Automatica*, 1999, 35. p.669-678.

[9] W. Wang, J. Yi, D. Zhao and D. Liu "Design of a stable sliding-mode controller for a class of second-order underactuated systems", *IEE Proc. Control Theory Appl.*, vol. 151, no. 6, 2004, pp.683-690.

[10] Ho-Hoon Lee, Yi Liang Del Segura "A Sliding-Mode Antiswing Trajectory Control for Overhead Cranes With High-Speed Load Hoisting", *ASME*,vol.128,pp. 842-845, Dec. 2006.

[11] K. Ohnishi, M. Shibata, and T. Murakami "Motion control for advanced mechatronics", *IEEE/ASME Trans.Mechatronics*, vol. 1, no. 1, pp. 56-67,Mar. 1996.

[12] A. Sabanovic, M. Elitas, and K. Ohnishi "Sliding modes in constrained systems control", *IEEE Trans. Ind. Electron.*, vol. 55, no. 9, pp. 3332-3339, Sep. 2008.

[13] M. H. Park and K. S. Kim "Chattering reduction in the position control of induction motor using the sliding mode", *IEEE Trans. Power Electron.*, vol. 6, no. 3, pp. 317-325, Jul. 1991.

[14] LEE, H.-H "Modeling and control of a three dimensional overhead crane", *ASME Transactions, Journal of Dynamic Systems, Measurement and control*, **120**, 471-476, 1998

[15] W. Wang, J. Yi, D. Zhao and D. Liu "Design of a stable sliding-mode controller for a class of second-order underactuated systems", *IEE Proc.-control Theory Appl.*, Vol. 151 683-690, 2004

[16] John J. Craig "Lyapunov stability", *Introduction to Robotics: Mechanics and Control*, Addison-Wesley Publishing Company, 3rd Edition, 2003, p 449-456.

[17] Ho-Hoon Lee "A new design approach for the anti-swing trajectory control of overhead cranes with high-speed hoisting", *International Journal of Control*,77: 10,931-940, 2004.

[18] John J. Craig "Chapter5 Path and trajectory planning", *Introduction to Robotics: Mechanics and Control*, Addison-Wesley Publishing Company, 3rd Edition, 2003, p 186-196.

[19] H. Ishino and T. Murakami "Anti Swinging Control of Automatic Crane System with Variable Rope Length", *8th France-Japan and 6th Europe-Asia Congress on Mechatronics* ,Nov, 2010